DESIGN PROCEDURE AND EXPERIMENTAL EVALUATION OF PRESSURE-SWIRL ATOMIZERS

Pedro Teixeira Lacava*, Demétrio Bastos-Netto, Amílcar Porto Pimenta***
***Instituto Tecnológico de Aeronáutica – Brazil**
****Instituto Nacional de Pesquisa Espaciais - Brazil**

Keywords: *pressure-swirl atomizer, liquid atomization.*

Abstract

In the pressure-swirl atomizer a swirling motion is imparted to the fuel, leading it under the action of the centrifugal force, to spread out in the form of a hollow cone as soon as it leaves the exit orifice. This kind of atomizer finds its use in gas turbines and liquid propellant rockets. The need to minimize the combustor length usually leads to a spray angle of around 90°. The present work suggests a procedure for designing a pressure-swirl atomizer. The droplets Sauter Mean Diameter (SMD) and the spray cone angle are evaluated and made to fit the calculated atomizer dimensions. The SMD is estimated through the use of a model originally developed for fan-spray atomizers and extended for pressure-swirl atomizers. A pressure-swirl atomizer was manufactured following this design procedure. The discharge coefficient, the spray cone angle and the Sauter Mean Diameter were evaluated experimentally and compared with the theory used to design the atomizer. The spray Sauter Mean Diameter was measured with a laser scattering system.

1 Introduction

The liquid fuel injection process plays an important role in many aspects of combustion processes performance. To obtain the surface to mass high ratios in the liquid phase which lead to the desired very high evaporation rates, the liquid fuel must be fully atomized before being injected into the combustion zone.

Atomization is usually accomplished by spreading the fuel into a thin sheet to induce instability thus promoting its disintegration into ligaments which collapse into droplets due to surface tension action. The discharging of the fuel through orifices with specially shaped passages, leads the fuel to become a thin sheet from which ligaments and ultimately droplets are formed, and these resulting droplets will be distributed through the combustion zone in a controlled pattern and direction.

In applications where combustion rates must be high, such as, for example, in aircraft gas turbines (around 500,000 kJ/m^3.s), the spray angle must be high, around 90°, due to the need of minimizing the combustor length. This must be achieved by imparting a swirling motion to the emerging fuel jet. Much wider cone angles are achieved with pressure-swirl atomizers where, a swirling motion is imparted to fuel so that, under the action of centrifugal force, it spreads out in the form of a hollow cone upon leaving the exit orifice.

Figure 1 shows schematically a pressure-swirl atomizer. The liquid is fed to the injector through tangential passages giving the liquid a high angular velocity, and forming, in the swirling chamber, a liquid layer with a free internal surface, thus creating a gas-core vortex. The liquid then is discharged from the nozzle in the form of a hollow conical sheet which breaks up into small droplets.

As pressure-swirl atomizers play an important role in gas turbine and liquid-propellant rocket engine combustion processes, there are several theoretical and experimental results available on this kind of atomization technique. Lefebvre [1] has organized the then most important references on atomization and sprays, including some aspects of pressure-swirl atomizers design procedures, and presented some predictions on discharge coefficients, spray-cone angles and mean droplet sizes. The

work of Couto et al. [2] showed a theoretical formulation for estimating the Sauter Mean Diameter of droplets generated by pressure-swirl atomizers. This was done extending the model of Dombrowski and Johns [3] on the disintegration of viscous liquid sheets generated by fan-spray atomizers, the results comparing satisfactorily with available experimental data and other existing empirical models. Bazarov and Yang [4] have discussed the liquid-propellant rocket engine pressure-swirl atomizer dynamics and its relation with flow oscillations. Paula Souza [5] presented a design procedure and performed an experimental analysis of a coaxial pressure-swirl bi-propellant atomizer for liquid-propellant rocket engines. Jones [6] presented a design optimization of a large pressure-jet atomizer for furnace power plants. Lefebvre [7] discussed the application of pressure-swirl atomizers in gas turbine combustion chambers.

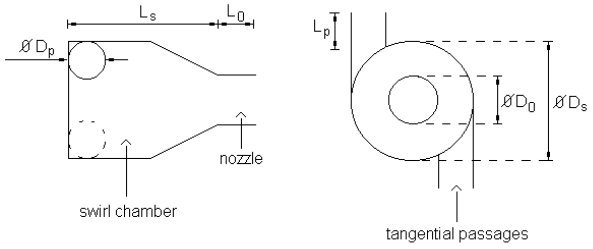

Fig. 1. Pressure-swirl atomizer schematics.

This work describes a procedure for designing a pressure-swirl atomizer. The Sauter mean diameter (SMD) and the spray cone angle are evaluated with the proper atomizer dimensions. The SMD is estimated using the formulation of Dombrowski and Johns, as extended by Couto et al. for pressure-swirl atomizers, as already mentioned. An atomizer was manufactured based on the suggested design procedure and its discharge coefficient, spray angle and SMD were measured and compared with the theoretical estimates of those parameters.

2 Design Considerations and Spray Predictions

The following data are required for an atomizer design: the liquid properties (density, surface tension, and viscosity), the discharging ambient characteristics (ambient pressure and density) and the liquid injection conditions (i.e., the mass flow rate and the injector pressure differential).

First the flow number, FN, is calculated using Equation (1):

$$FN = \frac{\dot{m}_L}{\sqrt{\rho_L \Delta P_L}} \qquad (1)$$

Where $\dot{m}_L$ is the liquid mass flow rate, ρ_L is the liquid density, and ΔP_L is the injector pressure differential.

The nozzle discharge diameter (D_0) (see Figure 1) must be chosen and the other remaining atomizer geometrical parameters are obtained considering the following dimensionless groups: $A_p/(D_s.D_0)$, D_s/D_0, L_s/D_s, L_0/D_0, and L_p/D_p; where the A_p is the tangential entry passage cross section area, and other important geometrical parameters are shown in Figure 1.

The ratio L_s/D_s should be reduced in order to minimize the wall friction losses. However, a limiting value is needed to achieve the liquid flow stabilization and formation of a uniform vortex sheet. This ratio must be higher than 0.5, and a typical value recommended for proper design is 1.0, as pointed out by Elkobt et al [8]. The parameter L_0/D_0 should also be reduced to minimize friction losses in the atomizer exit. Further, the ratio L_p/D_p cannot be smaller than 1.3 because a short tangential inlet passage channel may generate a diffuse discharge leading to an unstable spray (Tipler and Wilson [9]). Finally, one has to watch out for the obvious limitations of the manufacturing process itself

The others two dimensionless groups, i.e., $A_p/(D_s.D_0)$ and D_s/D_0, both have a considerable influence in the discharge coefficient, Cd, which can be calculated by the Equation (2).

$$Cd = \frac{\dot{m}_L}{A_0.\sqrt{2.\rho_L.\Delta P_L}} \quad (2)$$

The ratios $A_p/(D_s.D_0)$ and D_s/D_0 can be obtained from empirical relations for Cd developed by Carlisle [10], Risk and Lefebvre [11], and Jones [6], Equations (3), (4), and (5), respectively. In fact, the Cd calculated using the flow parameters in Equation (2), can be used to choose appropriates values for $A_p/(D_s.D_0)$ andD_s/D_0 with Carlisle result (Equation (3)), and the Cd is recovered with Risk and Lefebvre and Jones equations (i.e., Equations. (4) and (5), respectively) to check for discrepancies; Nevertheless intervals ranging from 0.19 to 1.21 and from 1.41 to 8.13 are recommended for $A_p/(D_s.D_0)$ and D_s/D_0, respectively (Lefebvre [1]).

$$Cd = \left(0.0616\frac{D_s}{D_0}.\frac{A_p}{D_s.D_0}\right) \quad (3)$$

$$Cd = 0.35.\left(\frac{D_s}{D_0}\right)^{0.5}.\left(\frac{A_p}{D_s.D_0}\right)^{0.25} \quad (4)$$

$$Cd = 0.45.\left(\frac{D_0.\rho_L.U_0}{\mu_L}\right)^{-0.02}.\left(\frac{L_0}{D_0}\right)^{-0.03}. \left(\frac{L_s}{D_s}\right)^{0.05}.\left(\frac{A_p}{D_s.D_0}\right)^{0.52}.\left(\frac{D_s}{D_0}\right)^{0.23} \quad (5)$$

Equation (5) reported by Jones [6], is the most elaborated one, showing that the ratios $A_p/(D_s.D_0)$ and D_s/D_0 are the dominant dimensionless parameters in the calculation of Cd.

In the present design procedure, the critical atomizer dimensions are accepted or not, depending on the calculated values of the spray semiangle (θ) and the mean drop diameter. The semiangle (θ) can be estimated by the expression developed by Giffen and Muraszew [12] for a pressure-swirl atomizer**:**

$$\sin\theta = \frac{(\pi/2).Cd}{K.(1+\sqrt{X})} \quad (6)$$

where $K = A_p/(D_s.D_0)$ and X is the ratio between the air core area (A_a) and the nozzle orifice exit area (A_0) , estimated by Equation (7) below**:**

$$D_0 = 2.\sqrt{\frac{FN}{\pi.(1-X).\sqrt{2}}} \quad (7)$$

With the flow number (FN) and the spray cone semiangle (θ), obtained from Equations (1) and (6), it is possible to estimate the liquid sheet thickness at the nozzle tip, h_0, as suggested by Couto et al. [7].

$$h_0 = \frac{0.00805.FN.\sqrt{\rho_L}}{D_0.\cos\theta} \quad \text{(MKS units)} \quad (8)$$

Dombrowski and Johns [3] derived an expression for estimating the ligament diameter, D_L, formed on the liquid film break up of a thin plane sheet atomizer as the one generated by a fan-spray atomizer. Couto et al. [2] extended this result for a pressure-swirl atomizer. They assumed that the conical sheet possesses, a rupture radius much larger than its thickness, that once the conical sheet is established, the amplitude of any disturbance (ripple) away from the injector tip is much smaller than the cone diameter (so that the ripple “sees” the conical sheet as a plane sheet) and that the wavelength of any ripples formed in the liquid film grows until its amplitude is equal to the ligament radius, so that one droplet is produced per wavelength. Then, the ligament diameter is given by

$$D_L = 0.9615 \cos\theta \left(\frac{h_0^4 \sigma^2}{U_0^4 \rho_a \rho_L} \right)^{1/6} . \left[1 + 2.6 \mu_L \cos\theta \left(\frac{h_0^2 \rho_a^4 U_0^7}{72 \rho_L^2 \sigma^5} \right)^{1/3} \right]^{0,2} \quad (9)$$

where σ (dyne/cm) is the liquid surface tension, ρ_a (g/cm^3) is the density of the surrounding medium, here taken to be the air in the combustion chamber, μ_L (cp) is the liquid dynamic viscosity, and U_0 (cm/s) is the velocity of the liquid at the atomizer tip, given by Equation (10).

$$U_0 = \sqrt{\frac{2.\Delta P_L}{\rho_L}} \quad (10)$$

According to Rayleigh mechanism (in Lefebvre [1]), assuming that the collapse of a ligament with diameter D_L will generate a droplet, then one may write (Couto et al [2]):

$$SMD = 1.89\, D_L \quad (11)$$

If the semiangle θ and the *SMD* estimated above are not adequate for the atomizer purposes, then a new set of dimensions must be chosen.

A water pressure-swirl atomizer with four tangential passages was designed and constructed following the procedure above described. Table1 displays the atomizer design input parameters.

Table 2 shows the results obtained in the above described calculations and the atomizer final dimensions. For the given input conditions, the combination θ = 34.89^o and *SMD* = 45.4 μm seems quite acceptable for combustion purposes**.** These dimensions were adjusted to simplify the atomizer construction**.** Nevertheless, the design boundaries above described for the dimensionless groups were strictly respected.

Tab. 1. Atomizer design input parameters.

ρ_L	1.00E+03 kg.m^3
μ_L	1.00E-01 kg.m^{-1}.s^{-1}
σ	7.34E-02 kg.s^{-2}
ρ_a	1.00E+00 kg.m^3
$\dot{m}_L$	6.00E-03 kg.s^{-1}
ΔP_L	4.00E+05 Pa
D_0	1.00E-03 m

Tab. 2. Final results for the atomizer design.

FN	3.00E-07 m^2	L_0/D_0	1.00
X	7.30E-01	L_p/D_p	1.60
h_0	9.31E-05 m	D_0	1.00 mm
U_o	28.28 m.s^{-1}	D_s	3.00 mm
D_L	24.00 μm	L_s	3.00 mm
SMD	45.40 μm	L_0	1.00 mm
Cd (Equation 7)	0.27	A_p	1.20 mm^2
$A_p/(D_s.D_0)$	0.40	D_p	0.60 mm
D_s/D_0	3.00	L_p	1.00 mm
L_s/D_s	1.00	θ	34.89^o

3. Experimental Setup

The liquid flow to the atomizer is kept by nitrogen pressurization and Figure 2 describes the experimental setup.

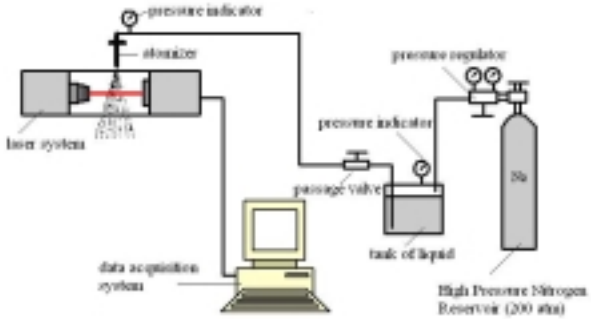

Fig. 2. Experimental setup.

To visualize the liquid film break up and to measure the semiangle (θ), a commercial Mavica – Sony MVC-FD97 camera was used

utilized. Initially a minimum exposure time and automatic flash were used to obtain the best possible instant picture. Then a maximum exposure time and no flash were used in order to obtain the spray mean boundaries.

Using the Photoshop® software, the pictures with longer exposure time were converted to negative form, in order to improve clarify the spray boundaries. Then, using the Autocad® software, the sprays half angles were determined.

A laser scattering system (Malvern Mastersizer X®) was used to analyse the spray droplet size distribution and the Sauter mean diameter (SMD). When the droplets go through the helium-neonium laser beam (633 nm), the circular photodiode detectors plate collects the laser scattered beam in angular sectors. To obtain the droplet size distribution, the system uses the Fraunhofer diffraction theory, i.e., the scattering angle is related to the droplet diameter. The scanning time is 2ms and each measurement corresponds to 2000 scans operations. Figure 3 shows the atomizer coupled to the laser system and the laser beam travelling through the spray.

The atomizer was assembled in a 3D positioning system, which was needed necessary to determine the best relative distance between the atomizer nozzle discharge orifice and the center line of the laser beam. The chosen distance was 4.0 cm, as this is the minimum distance for an adequate obscurescence level to be attained. For shorter distances, the obscurescence level is so high for the laser beam travelling closer to the atomizer, that, no light signal can be detected by the photodiodes.

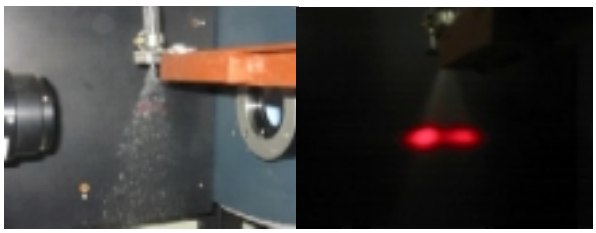

(a) (b)

Fig. 3. (a) Atomizer coupled to the laser system; (b) laser beam travelling through the spray.

To obtain the injector discharge coefficient, sprays under different operating pressures were discharged into a reservoir resting on a scale. The time taken to fill this reservoir with 2.0 kg of water was measured so that a mean liquid mass flow rate could be obtained. Then, substituting the values of the injector pressure differential and the mean mass flow rate readings in Equation (2), the experimental discharge coefficient was estimated.

3. Results

The pressure differential applied through the injector ranged from 2 atm to 6 atm. Under 2 atm, the liquid discharge did not generate a typical spray, but only a smooth film was formed around a hollow bubble resembling an onion; i.e., of no practical interest. On the other side, 6 atm was the limiting pressure for the reservoir.

Figure 4 shows (a) the liquid mass flow rate and (b) the discharge coefficient, both as functions of injector pressure differential. Figure 4 (b) also shows the Cd used in the injector design and calculated with Carlisle, Lefebvre and Risk and Jones equations (Equations 3, 4 and 5, respectively). The experimental results consist on the mean value of twenty scans, and it is possible to notice that the experimental results are quite close to the design values. For instance, at the design pressure differential of 4 atm, the mass flow rate and the discharge coefficient were 6.13 g/s and 0.2728, respectively, quite close to the design values of 6 g/s and 0.2700, respectively.

The liquid film breakup as a function of the pressure differential can be visualized in the short exposition time pictures presented in Figure 5. It is possible to observe that, in all test runs, a smooth liquid film around a hollow core was formed immediately after the atomizer nozzle exit orifice, ending in a ragged edge, and after that a well-defined hollow-cone spray was established. It is also possible to notice that the spray angle increases when the pressure differential increases, and the liquid film length is reduced. Figure 6 displays the spray

semiangle as a function of the pressure differential, obtained from pictures with long exposition time. According to Table 1, the theoretical prediction for the semiangle θ is 34.89° at the design conditions (for ΔP_L = 4 atm), close to the experimental result, of 34.5°.

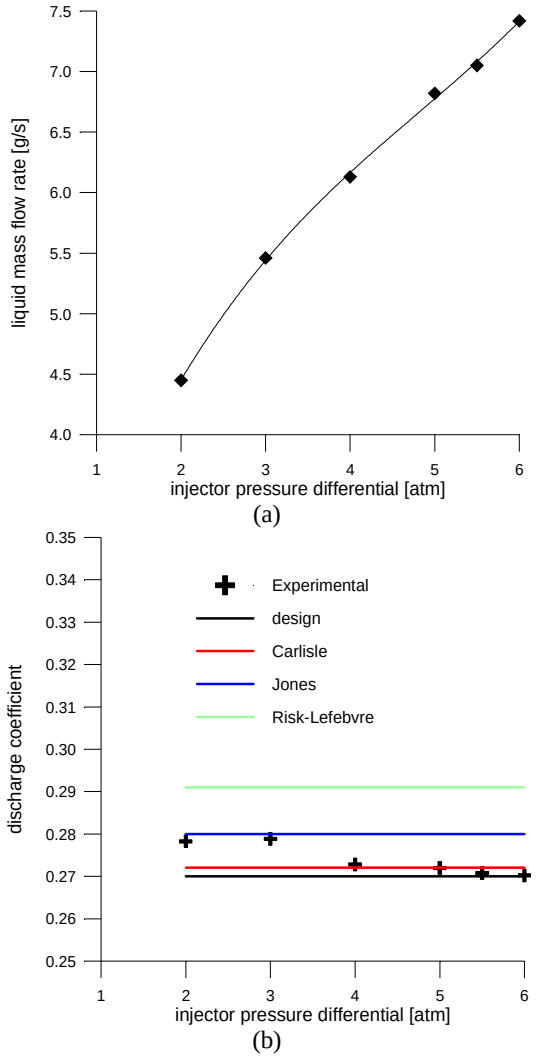

Fig. 4. The liquid mass flow rate (a) and the discharge coefficient (b), as functions of the injector pressure differential.

Figure 6 shows the spray semiangle increasing as the injector pressure differential increases, which is expected for the injector was not changed, i.e., it was kept with the same dimensions, and the mass flow rate also increases with the injector pressure differential as it was shown in Figure 4(a). Lefebvre [1], based upon theoretical and experimental investigations mentioned that, the spray angle is an inverse function of the injection pressure. However, this was so because in those investigations the injection pressure was analyzed in an isolated manner, the mass flow rate was kept constant and the injector dimensions were adjusted to fit the desired condition, i.e., a completely different case form the one performed here.

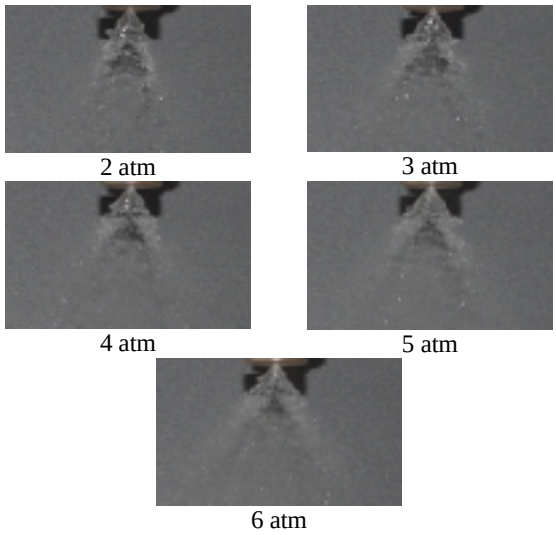

Fig. 5. Short exposition time for different injection pressures.

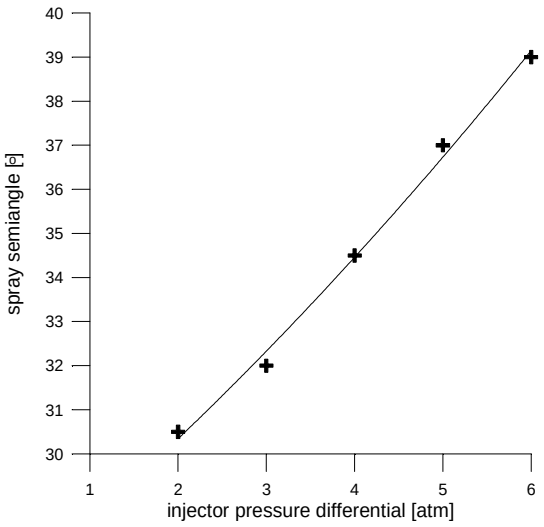

Fig. 6. Spray semiangle as a function of the injector pressure differential.

Figure 7 shows the experimental results of SMD measurements. Each experimental value presented in Figure 7 is the mean value of twenty scans, and repeatability was very satisfactory, with a maximum standard deviation 0,96% for 2.0 atm. The raising of the atomizer pressure differential is beneficial to the SMD as clearly illustrated in Figure 7 for the increasing in the liquid pressure differential causes the liquid to be discharged from the nozzle at higher velocity, promoting a thinner spray. The experimental behavior of the SMD with the injector pressure differential, ΔP_L , is typical of pressure swirl atomizers and it fully agrees with the tendency pointed out by other authors, such as, for example, Wang and Lefebvre [13].

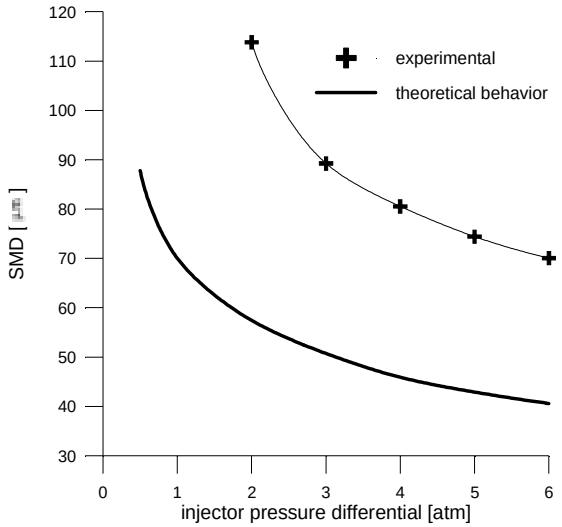

Fig. 7. Experimental and theoretical SMD as function of pressure differential.

Figure 7 also shows the prediction of the SMD using the equations presented in section 2. Clearly it is observed the theoretical curve has the same qualitative behavior of the experimental results (indeed they are nearly parallel to each other); however, the experimental values are 1.75 times the predicted ones. The theory applied to the calculated SMD assumed the atomization process to be in the fully developed spray stage, meaning that the curved surface formed immediately after the discharge orifice straightens to form a conical sheet**;** then, as the sheet expands, its thickness is reduced becoming unstable and disintegrating into ligaments which collapse by action of the surface tension into droplets thus generating a hollow cone spray. However, the pictures presented in Figure 5, indicate that the spray is still in a transition process from the "tulip" stage to the fully developed spray stage, due to the existence of a the smooth film in the immediate neighborhood of the injector exit section, as mentioned earlier. Then, as the droplets formed in the ragged edge at the end of the liquid film will be larger than those ones formed by the ligaments disintegration (Lefebvre [1]), it should be expected the experimental SMD to be larger than the predicted one.

In spite of the SMD importance to verify the spray quality, this is not enough, for it is necessary to make some considerations on the droplet diameter distribution behavior**.** Figure 8 presents the percentage of total droplets volume for different pressure differentials. The values were obtained directly from the data acquisition and statistical treatment software, and they were separated into three ranges of droplet diameters: 0 to 19μm, 20 to 100μm and higher than 100μm. Droplets with less than 19μm usually have low penetration and cause fuel concentration in regions close to the atomizer. High fuel concentration reduces the reactants mixing level, being a primary cause of increased soot formation and exhaust smoke. The second range, i.e., droplets in the 20 to 100μm range, is the best interval for liquid fuel combustion processes, due the more adequate penetration and the droplet diameters are sufficient for rapid vaporization in the combustion chamber. Droplets with more than 100μm have longer vaporization time, increasing the length of the mixing and burning regions.

Figure 8 also displays a well-defined droplet size distribution behavior as a function of the liquid pressure differential. The tendency is such that, when the pressure increases**,** the percentage of droplets with diameter smaller than 100μm also increases. The percentage of droplets in the 0 – 19μm range also increases;

but not as significantly as the percentage of the droplets larger than 100μm is reduced. However, even with a liquid pressure differential of 6 atm, a situation for which the SMD seems to be quite adequate for combustion purposes, the percentage of droplets larger than 100μm is relatively high, 42% of the total droplets volume. This can be a problem for situations requiring a high combustion rate, eventually leading to a combustion dispersion zone. Actually, this is not a function of the droplet size distribution only, but of a set of factors that influence the reactants mixing process and the combustion development itself. Therefore, an atomizer performance can be fully evaluated under actual combustion conditions only.

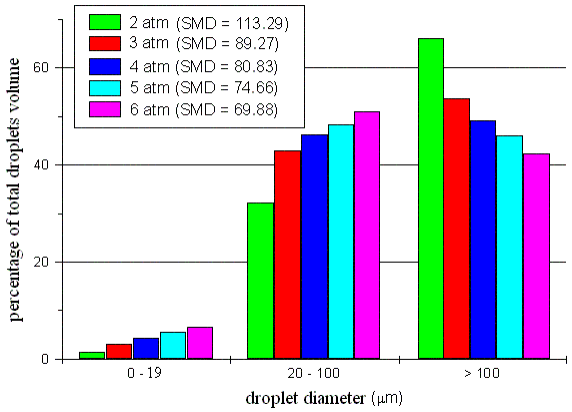

Fig. 8. Percentage of total droplets volume distribution among different pressure differentials.

Table 4 compares some theoretical and experimental atomizer parameters for ΔP = 4atm. The disagreement in the SMD values has already been discussed above.

Tab. 4. Comparison between the theoretical and experimental values for some atomizer parameters.

	$\dot{m}_L$	Cd	θ	SMD
Theoretical	6.00 g/s	0.2700	34.89°	45.40 μm
Experimental	6.13 g/s	0.2728	34.50	80.83 μm

4. Conclusions

It has been described here a pressure-swirl atomizer design methodology based on previous works. The SMD and the spray cone angle were evaluated during the process accepting the calculated atomizer dimensions. The liquid mass flow rate, the discharge coefficient, the spray semiangle, the SMD and the droplet size distribution were obtained experimentally to better evaluate the spray behavior and for comparison with the theoretical results from the design methodology.

Exception made for the SMD, the other experimental parameters agreed very well with the theoretical ones obtained in design methodology at the design point (ΔP = 4.0 atm). The spray visualization showed the presence of a smooth liquid film prior to the droplets formation, for all investigated pressure differentials, characterizing a transition from the "tulip" stage to the fully developed spray stage, increasing the presence of larger. The Dombrowski and Johns model extended by Couto et al. for pressure-swirl atomizers, assumes the droplets formation from a well established conical sheet at the final discharge orifice, not formed in the ragged edge at the end of the liquid film. This may be the reason for the SMD discrepancy. Figure 7 roughly suggests that for pressures higher than 6 atm, there might be a tendency to better agreement. However, this remains to be seen.

In this work only one atomizer was investigated and this was done in a limited range of injector pressure differentials, for the intent was the comparison of parameters at the design point (ΔP = 4 atm). Hence, for more conclusive results it would be interesting to compare different design conditions.

References

[1] Lefebvre A H. *Atomization and Sprays*. Hemisphere Publishing Corporation, New York, 1989.

[2] Couto H S, Carvalho Jr. J A and Bastos-Netto D. Theoretical Formulation for Sauter Mean Diameter of Pressure-Swirl Atomizers. *Journal of Propulsion and Power*, Vol. 13, No. 5, pp. 691 – 696, 1987.

[3] Dombrowski N and Johns W R. The Aerodynamic Instability Disintegration of Viscous Liquid Sheets. *Chemical Engineering Science*, Vol. 18, No. 2, pp. 203 – 214, 1963.

[4] Bazarov V G and Yang V. Liquid-Propellant Rocket Engine Injector Dynamics. *Journal of Propulsion and Power*, Vol. 14, No. 5, pp.797 – 806, 1998.

[5] Paula Souza J R. Estudo de um Injetor Centrífugo Bipropelente utilizado em Motor Foguete a Propelente Líquido (Thesis in Portuguese), *Instituto Tecnológico de Aeronáutica*, São José dos Campos, Brazil, 2001.

[6] Jones A R. Design Optimization of a Large Pressure-Jet Atomizer for Power Plant. *Proceedings of the 2nd International Conference on Liquid Atomization and Spray Systems, Madison*, Wis., pp. 181 – 185, 1982.

[7] Lefebvre A H. *Gas Turbine Combustion*. Hemisphere Publishing Corporation, New York, 1983.

[8] Elkotb M M, Rafat N M and Hanna M A. The Influence of Swirl Atomizer Geometry on the Atomization Performance. *Proceedings of the 1st International Conference on Liquid Atomization and Spray Systems*, Tokyo, pp. 109 – 115, 1978.

[9] Tipler W and Wilson A W. Combustion in Gas Turbines. *Proceedings of the Congress International des Machines a Combustion (CIMAC)*, Paris, pp. 897 – 927, 1959.

[10] Carlisle D R. Communication on the Performance of a Type of Swirl Atomizer, by A. Radcliffe. *Proc. Inst. Mech. Eng*., Vol. 169, p.101, 1955.

[11] Risk N K and Lefebvre A H. Internal Flow Characteristics of Simplex Swirl Atomizers. *Journal of Propulsion Power*, Vol. 1, No. 3, pp.193 – 199, 1985.

[12] Giffen E and Muraszew A. *Atomization of Liquid Fuels*, Chapman & Hall, London, 1953.

[13] Wang X F and Lefebvre A H. Mean Drop Sizes From Pressure Swirl Nozzles. *Journal of Propulsion Power*, Vol. 3, No. 1, pp. 11 – 18, 1987.